

Day-Ahead Dispatch of Liquid Air Energy Storage Coupled with LNG Regasification in Electricity and LNG Markets

Hooman Khaloie, *Graduate Student Member, IEEE*, and François Vallée, *Member, IEEE*

Abstract—Roadmaps toward a low-carbon renewable energy industry demand substantial bulk energy storages to account for non-dispatchability of renewables. Liquid Air Energy Storage (LAES) has gained recognition as one of few bulk-scale energy storage facilities not limited by geographical requirements, unlike pumped hydro and compressed air energy storage systems. However, the comparatively low efficiency of freestanding LAES facilities hinders their widespread stationing in power and energy systems. There has been a recent uptick of interest in the potential efficiency gains of coupling LAES with the Liquefied Natural Gas (LNG) regasification process. Thus, for the first time, this paper presents a day-ahead dispatch model for a LAES coupled with an LNG regasification process (hereafter, LAES-LNG), interacting with electricity and LNG markets as involved energy carriers. Through opportune sequence-aware LNG and electricity procuring, the coupled facility can benefit not only from the released cold energy during the LNG regasification process but also from co-firing regasified air and natural gas to produce and sell electricity. Focusing on a realistic market environment, the proposed dispatch model is derived as a two-stage stochastic setup. The cost-effectiveness of the proposed LAES-LNG facility is validated through a short-term daily test and a probabilistic economic feasibility study.

Index Terms—Electricity and Liquefied Natural Gas (LNG) markets, Liquid Air Energy Storage (LAES), LNG regasification, probabilistic payback period analysis, optimal dispatch.

NOMENCLATURE

A. Indices and sets

- $d \in \mathcal{D}$ Index and set of electricity market scenarios.
 $l \in \mathcal{L}$ Index and set of LNG market scenarios.
 $t \in \mathcal{T}$ Index and set of time periods within the dispatching horizon.

B. Parameters

- ER Energy ratio of the facility, $[\frac{\text{MWh}_{\text{in}}}{\text{MWh}_{\text{out}}}]$.
 HR Heat rate of the facility, $[\frac{\text{MWh}_{\text{thermal}}}{\text{MWh}_{\text{out}}}]$.
 k_t Duration of time period t , [h].
 LHV Lower heating value of LNG, [MJ/kg].
 $\overline{\mathcal{P}}^{\text{ch}}$ Upper bound of charged electricity, [MW].
 $\underline{\mathcal{P}}^{\text{ch}}$ Lower bound of charged electricity, [MW].
 $\overline{\mathcal{P}}^{\text{dis}}$ Upper bound of discharged electricity, [MW].
 $\underline{\mathcal{P}}^{\text{dis}}$ Lower bound of discharged electricity, [MW].
 q_0^{LNG} Initial liquid level of the LNG storage, $[\text{m}^3]$.
 q_0^{LAES} Initial liquid level of the liquid air tank, [MWh].

- $\overline{Q}^{\text{LNG}}$ Upper bound of liquid level in LNG storage, $[\text{m}^3]$.
 $\underline{Q}^{\text{LNG}}$ Lower bound of liquid level in LNG storage, $[\text{m}^3]$.
 $\overline{Q}^{\text{LAES}}$ Upper bound of liquid level in liquid air tank, [MWh].
 $\underline{Q}^{\text{LAES}}$ Lower bound of liquid level in liquid air tank, [MWh].
 \mathcal{R}^{LNG} Boil-off rate of the LNG storage, $\in [0, 1]$, $[\text{day}^{-1}]$.
 $\mathcal{R}^{\text{LAES}}$ Boil-off rate of the liquid air tank, $\in [0, 1]$, $[\text{day}^{-1}]$.
 η Efficiency of the regasification unit, $\in [0, 1]$.
 ϑ^{ch} Variable operation and maintenance cost during charging mode, [€/MWh].
 ϑ^{dis} Variable operation and maintenance cost during discharging mode, [€/MWh].
 $\lambda_{d,t}^{\text{Elec}}$ Electricity price in day-ahead electricity market, [€/MWh].
 λ_l^{LNG} LNG price in day-ahead LNG market, [€/MWh].
 ξ^{ℓ} Loading capacity of the LNG storage, $[\text{m}^3/\text{h}]$.
 ξ^{ρ} Unloading capacity of the LNG storage, $[\text{m}^3/\text{h}]$.
 ϖ LNG weight per unit volume, $[\text{kg}/\text{m}^3]$.
 ρ Correlation coefficient between investment cost and annual profit, $\in [-1, 1]$.
 $\overline{\Psi}^{\text{LNG}}$ Upper bound of daily bought LNG, [MWh].
 $\underline{\Psi}^{\text{LNG}}$ Lower bound of daily bought LNG, [MWh].

C. Variables

- G Payback period following a Gaussian distribution, [year(s)].
 h_t Quantity of LNG bought from day-ahead LNG market, [MW].
 H^{tot} Total daily bought LNG, [MWh].
 $P_{l,d,t}^{\text{dis}}$ Quantity of electricity discharged (sold) to the day-ahead electricity market, [MW].
 $P_{l,d,t}^{\text{ch}}$ Quantity of electricity charged (bought) from the day-ahead electricity market, [MW].
 $q_{l,d,t}^{\text{LNG}}$ Liquid level of the LNG storage, $[\text{m}^3]$.
 $q_{l,d,t}^{\text{LAES}}$ Liquid level of the liquid air tank, [MWh].
 X Total investment cost following a Gaussian distribution, [€].
 Z Annual profit following a Gaussian distribution,

	[€/year].
$\alpha_{l,t}^{\text{dis}}, \alpha_{l,t}^{\text{ch}}$	Binary variable modeling discharging and charging behaviors of the LAES plant, $\in \{0,1\}$.
$\beta_{l,t}^{\text{dis}}, \beta_t^{\text{ch}}$	Binary variable modeling discharging and charging behaviors of the LNG storage, $\in \{0,1\}$.
μ_g	Mean of <i>payback period</i> , [year(s)].
σ_g	Standard deviation of <i>payback period</i> , [year(s)].

D. Functions

$\mathcal{F}(y, \theta_l, \theta_d)$ Profit function of the LAES-LNG facility with y , θ_l , and θ_d as the vector of decision variables, LNG and electricity market scenarios, respectively.

$f(g)$ Probability density function of *payback period*.

$a(g), b(g)$ Arbitrary functions related to $f(g)$.

$m, n(g)$ Arbitrary functions related to $f(g)$.

$\Theta(\psi)$ Error function evaluated for ψ .

I. INTRODUCTION

A. Motivation and Background

BULK, or large-scale, energy storages are indispensable elements of future energy networks approaching 100% share of intermittent renewable energy. The rising contribution of intermittent renewables into energy networks entails deploying colossal flexibility sources, e.g., bulk energy storages, to retain real-time supply and demand equilibrium through peak shaving or load leveling. Driven by recent studies, merely pumped hydro and compressed air energy storages encompass sufficient maturity among all existing energy storages for bulk-scale grid applications [1]. Pumped hydro storages are recognized as high-efficient and cost-effective bulk storages that can only be built in specific locations with favorable geological features, though most viable areas have been already erected and exploited. On the other hand, compressed air energy storage is another fairly efficient technology that demands: 1) gigantic above-ground air storage tanks, requiring significant investment costs, or 2) natural underground caverns that charge geographical limitations [2]. Needless to say, electrochemical energy storages like lithium-ion and flow batteries are best suited for small- and medium-scale grid applications, such as frequency control services [3].

The foregoing obstacles have drawn increasing attention to Liquid Air Energy Storage (LAES)¹, that lends itself well to bulk-scale applications. Since liquefied air with high energy density is leveraged as the working fluid in the LAES facility, considerably smaller storage tanks are required, resulting in reduced initial investment costs. Furthermore, the LAES is restricted to no geographical or geological constraints, making it more amenable to industrialization and grid integration purposes [4]. Also, similar to compressed air energy storage, LAES is deemed a potentially suitable asset for sector coupling or integrating multiple energy carriers [5].

The development of LAES may be broken down into a number of turning points along the way. The origin of storing

energy via liquid air can be traced back to 1977 [6], but it was not until years later that Mitsubishi Heavy Industries conducted practical research into the notion [7]. With an eye to storing electricity through liquid air, the University of Birmingham is home to the first LAES pilot facility, developed between 2009-2012, with power and energy storage capacities of 350 kW and 2.5 MWh, respectively. In 2018, a 5 MW/15 MWh demonstration-scale LAES facility was launched in Manchester, leading to the first commercial 50 MW/300 MWh LAES project set for grid connection in Northern England during 2023-2024 [8], [9]. The project is being developed by Highview Power, a UK-based company that specializes in cryogenic energy storage facilities [9]. Highview Power is currently at the forefront of commercial LAES projects worldwide, leading the way in their implementation. The company has an extensive portfolio of LAES projects under development across the globe, including a 200 MW/2.5 GWh facility in Yorkshire [9], UK, a 50 MW/400 MWh facility in Vermont, USA [10], seven 50 MW/300 MWh facilities in Spain [11], and a 50 MW/600 MWh facility in Chile [12].

B. Literature Review on the LAES Dispatch Problem

With the recent surge in the popularity of the LAES, studies focusing on the optimal interaction of LAES with electricity markets to make profits have emerged as an interesting line of research. Prior research has examined the LAES dispatch problem from the perspective of either a freestanding facility [13]–[17], or LAES plants supplemented with other resources, such as photovoltaic or air separation systems [18]–[20].

As one of the first works on the dispatch of freestanding LAES, Khani and Dadash Zadeh [13] proposed a mixed-integer linear weekly scheduling model for a LAES facility under deterministic point forecasts in a real-time electricity market. The authors proposed subsidizing LAES investors via electricity price modulation as an incentive program, although large modulation factors are necessary to provide the desired income for investors. An energy and reserve market-focused techno-economic study of a LAES facility was undertaken by Xie *et al.* in [14]. Half-hourly electricity prices and a genetic algorithm were employed for the economic study. In [15], a similar approach to that of [14] was developed for the dispatch of the LAES facility in the energy market under different operating (market bidding) strategies. Without realistically modeling the LAES dispatch problem in the electricity market, the authors discovered that the payback period of the LAES would be longer than its lifetime.

While the dispatch of freestanding LAES facilities under steady-state conditions has been the main focus of previous works [13]–[15], there has been a parallel research effort to incorporate LAES thermodynamics into the facility's scheduling problem [16], [17]. In this regard, a yearly linear schedule for a LAES facility in energy and ancillary services markets was presented by Vecchi *et al.* [16], which dealt with the plant's thermodynamic attributes. The authors realized that under the assumed market circumstances, storage capacities larger than 2-3 hours do not considerably affect the LAES revenue. Following on from [16], Vecchi *et al.* [17] conducted

¹Liquid Air Energy Storage (LAES) is a form of "cryogenic energy storage".

an economic feasibility study for a freestanding LAES facility interacting with energy and ancillary services markets with an eye on LAES off-design operation. The authors' findings conclusively revealed a significant relationship between the off-design performance of the LAES and delivered ancillary services.

Apart from the previous studies on freestanding LAES facilities, another area of research has emerged, which explores the dispatch strategies of LAES plants supplemented with other resources [18]–[20]. In [18], Legrand *et al.* presented an algorithmic scheduling strategy for a LAES facility and a photovoltaic power plant in the energy market, along with a techno-economic analysis. While providing some interesting insights for LAES sizing, the authors' endeavor may not ensure the optimality of the results since the dispatch problem was not designed as a mathematical optimization problem. Zhang *et al.* [19] evaluated the financial gains of introducing the LAES facility to a present air separation unit through mixed-integer linear programming in energy and reserve markets. The reserve demand uncertainty was modeled using confidence bound, and the model focused on weekly dispatch. Recently, Kong *et al.* [20] suggested a daily dispatch model for a LAES facility with an air separation unit. Significant financial gains were realized for the designed system by concentrating on time-of-day pricing rather than real-time pricing.

C. LAES Efficiency Improvement and Research Gaps

Despite the early mentioned benefits of the LAES [5], its ongoing deployments in energy networks [8], and evolving research [13]–[20], the comparatively low efficiency of freestanding LAES facilities is the main barrier to their widespread installation in power and energy networks. Although joint dispatching of renewable and air separation units alongside a LAES setup increases the system's flexibility [18]–[21], it does not affect LAES efficiency. Therefore, improving LAES round-trip efficiency has emerged as a crucial area of research, leading to exploring four general pathways and directions within this domain [5], [8].

The first pathway involves integrating LAES with external cold sources, such as the cold released during Liquefied Natural Gas (LNG) regasification process to aid air liquefaction during the charging mode [22]. The second strategy involves incorporating external heat sources, like co-firing natural gas with regasified air during discharging [23]. Third, integrating renewables like geothermal [24] and solar thermal [25] systems with LAES can improve power generation efficiency in LAES. Finally, hybridizing LAES with other energy storage technologies, such as pumped thermal energy storage, by sharing/replacing certain components or providing heat and cold sources, represents another promising avenue to enhance the efficiency of LAES [26]. While each pathway offers its specific advantages, significant focus has been placed on harnessing both external cold and heat sources to enhance LAES efficiency within charging and discharging modes [5], [8]. In pursuit of this objective, the integration of LAES with the LNG regasification process has emerged as a notable area

of research. This integration holds considerable potential, as highlighted in [27]–[29]. In this approach, (i) during LAES charging, the released cold energy from the LNG regasification is further leveraged in the air liquefaction, and (ii) during LAES discharging, the regasified air and natural gas are co-fired to power a gas turbine and generate electricity. As a result, by leveraging the first two pathways mentioned earlier, the performance of the LAES can be simultaneously enhanced, potentially leading to a competitive performance in the energy storage landscape. While thermodynamics and functionality of coupling LAES and LNG regasification process (hereafter, LAES-LNG) have been examined and validated in a broad body of literature [27]–[29], the following have remained open issues so far:

First, the optimal operation strategy of the LAES-LNG facility toward a cost-effective dispatch remains unexplored in the existing literature. Assuring the facility's financial feasibility requires a well-laid mathematical programming setup that has not been presented so far.

Second, in the context of the LAES-LNG facility, the trading platform involving both electricity and LNG as energy carriers remains uncovered in the relevant literature. While previous works in power system studies have extensively addressed the electricity market, studies involving LNG have primarily focused on its utilization as a natural gas provider [30], [31] or its integration into the natural gas market/network [32], [33], without delving into LNG market setups. Consequently, there is a notable gap in the literature concerning the LNG market as a fundamental component of LNG provision. Additionally, the optimal daily operation of the LAES-LNG facility requires a proper market-oriented sequence-aware decision-making framework in LNG and electricity markets that are usually cleared at different times of the day, which also has not been addressed before.

Third, although some economic indicators have been examined for the LAES-LNG facility in [27]–[29], the economic viability of the facility can not be assessed without a (i) well-laid optimal operation strategy for the LAES-LNG facility and (ii) proper market-oriented sequence-aware interaction with electricity and LNG markets as the involved carriers. In this regard, a proper economic feasibility study should be conducted to assess the LAES feasibility and its long-term potential for deployment in energy markets. Evaluating the *payback period*, which serves as a key metric for assessing economic feasibility, is an essential initial step in the process of LAES commercialization to determine the timeframe for recovering investment costs. While the *payback period* has not been analyzed for the LAES-LNG facility in [27]–[29], several studies have leveraged this metric to assess the economic viability of different LAES layouts [14]–[16], [18]. The *payback period* of the LAES is influenced by uncertain investment costs and annual profits, with the former attributed to the project's complex composition and susceptibility to market fluctuations, inflation, technological advancements, and unforeseen events, while the latter is affected by the high price volatility of the involved energy carriers. Earlier studies [14]–[16], [18] neglected these sources of uncertainty and treated them as fixed values, leading to a deterministic *payback period*

analysis.

D. Contributions and Paper's Structure

To shed light on the preceding challenges, this paper proposes a day-ahead dispatch model for a LAES-LNG facility in day-ahead electricity and LNG markets. This work makes the following contributions in detail:

- (i) For the first time, this paper puts forth an innovative mathematical setup designed specifically for the dispatch of a LAES-LNG facility. While the facility design has been the focus of several studies [27]–[29], this work extends the existing body of research by establishing a well-laid dispatch model of the LAES-LNG system.
- (ii) This is the first study proposing a new trading structure in day-ahead LNG and electricity markets in light of a real-life market setup, addressing the research gap in short-term LNG trading for power system studies. Further, to address the lack of research on sequence-aware participation in day-ahead LNG and electricity markets, where market closure times differ, the dispatch formulation presented in (i) is tailored to a two-stage stochastic model under uncertainty.
- (iii) To provide a more realistic and thorough assessment of the LAES long-term feasibility, this study advances previous research by conducting a probabilistic analysis of the *payback period*. In contrast to previous works, this analysis incorporates uncertainties in both investment cost and annual profit. Notably, this study is the first to undertake a *payback period* analysis under uncertainty within the LAES domain.

The remainder of this paper is broken up into five sections. Section II outlines the system description, market setup, and model assumptions. The day-ahead dispatch formulation is presented in Section III. Section IV discusses the economic feasibility study on the grounds of a probabilistic *payback period*. Multiple analyses and comparisons are performed in Section V. Finally, Section VI concludes the paper.

II. SYSTEM DESCRIPTION, MARKET SETUP, AND MODEL ASSUMPTIONS

This section is divided into three subsections. Subsection II-A provides a high-level overview of both freestanding LAES and LAES-LNG facilities. Market setup for both electricity and LNG is delineated in subsection II-B. Finally, model assumptions are given in subsection II-C.

A. System Description

Fig. 1 displays the layout of a freestanding LAES facility broken down into three primary subsystems: charging, storage, and discharging. Using grid-purchased electricity, the charging subsystem compresses air before delivering it to the liquefaction unit for transformation into a liquid state. The liquefied air is subsequently transferred to an atmospheric liquid air tank for storage. The discharging subsystem initially increases the pressure of the liquid air by pumping. The fluid then travels through the evaporator and expander (with

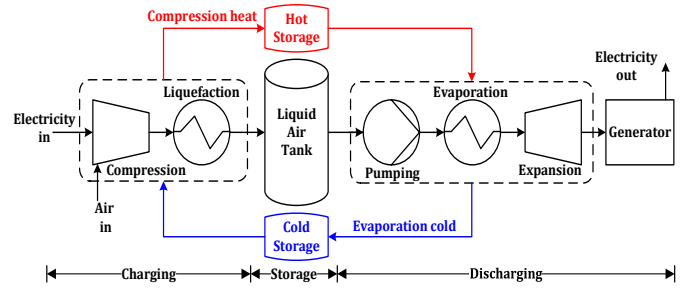


Fig. 1: Schematic layout of the freestanding LAES facility.

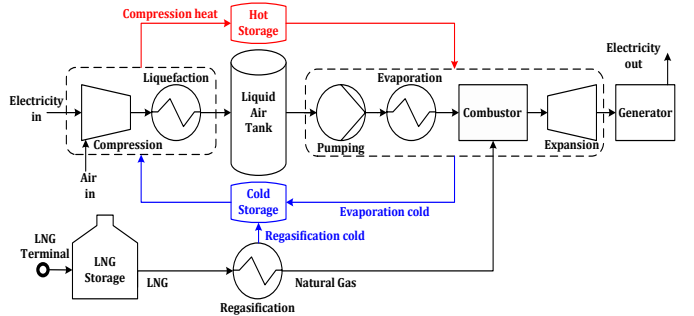


Fig. 2: Schematic layout of the proposed LAES-LNG facility.

several stages) to generate electricity. Needless to say, the released compression heat and evaporation cold energies are recovered and utilized in discharging and charging subsystems to increase the system's round-trip efficiency. Despite such utilization, the ultimate round-trip efficiency of freestanding LAES facilities is not competing. This has led to gaining widespread favor in integrating LAES with other processes, such as LNG regasification [27]–[29].

Fig. 2 shows the layout of the proposed LAES-LNG facility. In addition to the previously described subsystems (charging, storage, and discharging), the LAES-LNG facility contains three additional components: LNG storage, regasification unit, and combustor. These components play a crucial role in electricity and LNG coupling within the proposed facility. Like freestanding LAES, the charging subsystem is responsible for drawing electricity from the grid to compress the ambient air. Next, the liquefaction unit turns the compressed air into a liquid state and transfers the liquefied air to the liquid air tank. The required cold energy of the liquefaction unit is derived from two sources: the released cold energy from (i) liquid air evaporation and (ii) LNG regasification processes. This way, the electricity charging subsystem is coupled with the LNG regasification process. In the meantime, the authorized terminal supplies LNG to the LNG storage. When it comes to discharging electricity, liquefied air in the liquid air tank is pressurized and transferred to the combustor. Meanwhile, the LNG is passed through the regasification unit, and the resulting natural gas is conveyed to the combustor. The regasified air and natural gas are mixed and co-fired in the combustor to power a gas turbine through a high-temperature fluid and generate electricity. Thus, the energy flow between the LNG system and the LAES discharging subsystem is effectively interconnected.

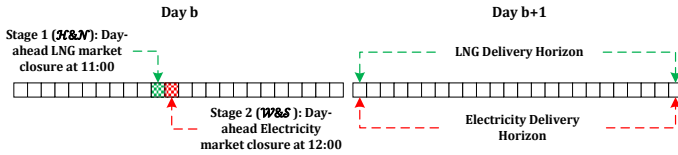


Fig. 3: Market setup for day-ahead electricity and LNG trading.

B. Market Setup

The day-ahead dispatch of the LAES-LNG facility requires well-suited interaction with involved energy carriers, namely, electricity and LNG. With the advent of deregulated energy markets worldwide, electricity and gas derivatives such as LNG can be traded daily to fulfil the needs of suppliers and consumers. Similar to the nature of many European energy markets, this study adopts the market setup embedded in Spain to analyze the economic feasibility of the LAES-LNG facility while being readily adaptable to other market structures. Therein, electricity and LNG are traded in the Iberian electricity market² and Iberian gas derivatives market³, respectively. Electricity and LNG are both traded one day in advance, whereas longer and shorter time frames are also available. A unique aspect of the Iberian gas derivatives market is that any market player can trade LNG in the *virtual balancing tank* (TVB⁴) without any physical limitation. Before the launch of TVB, the LNG transactions were unconcentrated and restricted to each LNG terminal/regasification plant. The TVB was launched in Spain on April 1, 2020, to eliminate physical limitations by consolidating the LNG storage capacity of all Spanish regasification plants into a single virtual tank. In other words, the TVB integrates all LNG terminals into one virtual LNG hub, allowing for dynamic adjustments in arrival and withdrawal patterns. The single virtual tank allows market participants to buy and sell LNG within the TVB without being constrained by the specific regasification plant where the LNG is physically stored, which increases the number of counterparties and enhances market liquidity and efficiency.

Market setup for day-ahead electricity and LNG trading are exhibited in Fig. 3. It is observed that the LNG market is cleared at 11:00 a.m., while the electricity market is cleared one hour later, i.e., at noon. Due to the market setup, the LAES-LNG facility must place its LNG bids for the next day in the LNG market before 11:00 a.m. Day-ahead LNG market results are released shortly after 11:00 a.m. (market closure), and in between, the LAES-LNG facility can submit its day-ahead electricity bids and offers⁵ before noon with perfect knowledge of LNG prices. Immediately after noon, the day-ahead electricity market results are released, and the next day's schedule for the LAES-LNG facility will be set.

²OMIE (Operador del Mercado Ibérico de Energía): <https://www.omie.es/>

³MIBGAS (Mercado Ibérico de Gas): <https://www.mibgas.es/>

⁴Tanque Virtual de Balance.)

⁵It is generally acknowledged that bids and offers in energy markets represent buying and selling quantities, respectively.

C. Model Assumptions

The considered day-ahead dispatch model for the LAES-LNG facility is built on the following assumptions:

- The facility's interaction with electricity and LNG markets is modeled as a perfectly competitive player with no market power under steady-state conditions.
- A two-stage stochastic program is developed to tackle sequential decision-making in uncertain day-ahead electricity and LNG markets, as delineated in Fig. 3. The uncertainties, i.e., LNG and electricity prices, are embodied under discrete scenarios generated by Gaussian distributions [34]. For a daily dispatching horizon, a set of 24 individual Gaussian distributions is utilized to generate electricity price scenarios, with each distribution corresponding to a specific period. In contrast, since the LNG price remains constant throughout the day, a single Gaussian distribution is employed to generate LNG price scenarios.
- The uncertainty in investment cost and annual profit is treated by Gaussian distributions for the economic feasibility study. Using probability distributions for these parameters allows decision-makers to comprehensively understand the range of possible costs and the corresponding probabilities, leading to more informed decision-making. When it comes to economic feasibility study and particularly the *payback period* analysis, it is crucial to address and account for inherent uncertainties in the annual profit and investment cost of the LAES-LNG facility, stemming from the volatility of electricity and LNG markets and the complex nature of cost estimation for infrastructure projects. Accordingly, it is widely acknowledged that economic variables, such as investment cost and profit, can be reasonably modeled as Gaussian distributions. This is due to (i) the central limit theorem (this theorem asserts that when many independent and identically distributed random variables are summed, the resultant distribution will approach a normal distribution) [35], (ii) extensive empirical evidence acknowledged that many economic variables, including investment cost and annual profit, roughly follow Gaussian distributions [36], [37], and (iii) the familiarity of engineers with Gaussian distributions attributed to its desirable analytical properties.

III. DAY-AHEAD DISPATCH FORMULATION

The day-ahead dispatch model for the LAES-LNG facility depicted in Fig. 2 is formulated in this section. For brevity, the formulation for day-ahead dispatch of the freestanding LAES facility shown in Fig. 1 is provided in the electronic companion of the paper, Appendix A (adapted from [13]). The market setup for such a dispatch model demands a sequential interaction with LNG and electricity markets. Therefore, a two-stage stochastic setup with the following sequence of decisions is designed to meet such a pressing need:

- 1) *Here-and-now* ($\mathcal{H}\&\mathcal{N}$) decisions: The facility must decide on its LNG bids for the next day before 11:00 a.m. of the present day. Thus, $\mathcal{H}\&\mathcal{N}$ (first-stage) decisions include LNG bids in the day-ahead LNG market to

receive LNG from the terminal and, consequently, the charging status of the LNG storage. It is worth noting that the LNG transfer from the LNG terminal to the LNG storage is not possible unless the LNG storage is in the charging status. Thus, the charging status of the LNG storage is linked to the LNG bids and is an $\mathcal{H}\&\mathcal{N}$ decision. This set of decisions must be made before the LNG market closure, i.e., 11:00 a.m.

- 2) *Wait-and-see* ($\mathcal{W}\&\mathcal{S}$) decisions: Shortly after 11:00 a.m., the day-ahead LNG market results are revealed, and in the meanwhile, the facility must decide on its day-ahead electricity bids and offers for the next day before the electricity market closure at noon. Therefore, $\mathcal{W}\&\mathcal{S}$ (second-stage) decisions contain bids and offers in the day-ahead electricity market. Notably, all remaining decisions of the LAES-LNG facility (e.g., discharging status of LNG storage and etc.) fall under the category of the second stage ($\mathcal{W}\&\mathcal{S}$).

The day-ahead dispatch model for the LAES-LNG facility is designed to maximize the facility's expected profit within a 24-hour dispatching horizon ($\mathcal{T} = 24$ hours) under the following two-stage stochastic setup:

$$\begin{aligned} \text{Max } \mathbb{E} \mathcal{F}(y, \theta_l, \theta_d) = & \\ \sum_{t \in \mathcal{T}} \left[\mathbb{E}_{\mathcal{H}\&\mathcal{N}} \left[\underbrace{-h_t k_t \lambda_l^{\text{LNG}}}_{\mathcal{O}_1} + \mathbb{E}_{\mathcal{W}\&\mathcal{S}|\mathcal{H}\&\mathcal{N}} \left[\underbrace{P_{l,d,t}^{\text{dis}} k_t \lambda_{d,t}^{\text{Elec}}}_{\mathcal{O}_2} \right. \right. \right. & \\ \left. \left. \left. \underbrace{-P_{l,d,t}^{\text{ch}} k_t \lambda_{d,t}^{\text{Elec}}}_{\mathcal{O}_3} - \underbrace{P_{l,d,t}^{\text{dis}} k_t \vartheta^{\text{dis}}}_{\mathcal{O}_4} - \underbrace{P_{l,d,t}^{\text{ch}} k_t \vartheta^{\text{ch}}}_{\mathcal{O}_5} \right] \right] \right] & \quad (1) \end{aligned}$$

where $\mathcal{F}(y, \theta_l, \theta_d)$ stands for the facility's profit function, y for the vector of decision variables, and θ_l and θ_d for the vector of LNG and electricity market scenarios, respectively. For each time period, defined by the time interval k_t between two successive periods (1 hour), term \mathcal{O}_1 represents the cost associated with LNG bids submitted to the day-ahead LNG market to load the LNG storage. In the relevant literature, this term is known as $\mathcal{H}\&\mathcal{N}$ or first-stage objective function since the involved decision variable does not depend on any scenario realization. In (1), term \mathcal{O}_2 accounts for the revenue of selling the generated electricity by the generator to the day-ahead electricity market. Term \mathcal{O}_3 derives the cost imposed on the facility for buying electricity to liquefy air and subsequently store it in the liquid air tank. Finally, terms \mathcal{O}_4 and \mathcal{O}_5 model the operational costs of the facility within discharging and charging modes, respectively. Last but not least, terms $\mathcal{O}_2 - \mathcal{O}_5$ shape the recourse function. The recourse function serves as a mathematical representation of the second-stage problem, wherein decisions are contingent upon realizing the LNG market price. Technical constraints of the LAES-LNG facility are detailed in the following.

Equation (2) specifies the total transferred LNG from TVB to the LNG storage within the dispatching horizon. According to the constraints set by the Iberian derivative gas market operator, the total daily value of LNG bids submitted by the facility should be kept within a given range, as modeled in (3). The market operator establishes this range to uphold

a consistent level of operational coherence and manageable conditions within the LNG market.

$$\sum_{t \in \mathcal{T}} h_t k_t = H^{\text{tot}}, \quad h_t \geq 0 \quad (2)$$

$$\underline{\Psi}^{\text{LNG}} \leq H^{\text{tot}} \leq \overline{\Psi}^{\text{LNG}} \quad (3)$$

The liquid level of LNG storage (quantity of presently stored liquid) at each period depends upon four factors: (i) the LNG liquid level at the previous period, (ii) the boil-off rate of LNG storage, (iii) the quantity of bought LNG, and (iv) the quantity of LNG discharged from the LNG storage to the regasification unit. Boil-off rate of LNG storage refers to the quantity of the LNG lost as gas owing to natural evaporation. In view of this, equations (4) and (5) draw the liquid level of LNG storage at the first and remaining periods, respectively:

$$\begin{aligned} q_{l,d,t}^{\text{LNG}} = q_0^{\text{LNG}} \left(1 - \frac{\mathcal{R}^{\text{LNG}}}{24} \right) + \frac{h_t k_t \times 3600}{\text{LHV} \times \varpi} - & \\ \frac{P_{l,d,t}^{\text{dis}} k_t \times \text{HR} \times 3600}{\eta \times \text{LHV} \times \varpi} \quad \forall t = 1, \forall l, \forall d & \quad (4) \end{aligned}$$

$$\begin{aligned} q_{l,d,t}^{\text{LNG}} = q_{l,d,t-1}^{\text{LNG}} \left(1 - \frac{\mathcal{R}^{\text{LNG}}}{24} \right) + \frac{h_t k_t \times 3600}{\text{LHV} \times \varpi} - & \\ \frac{P_{l,d,t}^{\text{dis}} k_t \times \text{HR} \times 3600}{\eta \times \text{LHV} \times \varpi} \quad \forall t \geq 2, \forall l, \forall d & \quad (5) \end{aligned}$$

In equations (4)-(5), 3600 is a conversion factor used to convert MWh to MJ. Constraint (6) states that the liquid level of LNG storage at the last period should be the same as the initial. Accordingly, constraint (7) ensures keeping the liquid level of LNG storage within its operational limits.

$$q_{l,d,t}^{\text{LNG}} = q_0^{\text{LNG}} \quad \forall t = 24, \forall l, \forall d \quad (6)$$

$$\underline{Q}^{\text{LNG}} \leq q_{l,d,t}^{\text{LNG}} \leq \overline{Q}^{\text{LNG}} \quad \forall t, \forall l, \forall d \quad (7)$$

The quantity of LNG transferred from the TVB to the LNG storage should never exceed the loading capacity of the LNG storage, as expressed in (8), to maintain the structural integrity of the storage. Conversely, the quantity of LNG discharged from the LNG storage to the regasification unit, as defined on the left side of constraint (9), must always remain below or equal to the maximum unloading capacity of the LNG storage. The operational constraint represented in (10) ensures the infeasibility of charging and discharging the LNG storage simultaneously.

$$0 \leq \frac{h_t k_t \times 3600}{\text{LHV} \times \varpi} \leq \xi^\ell \beta_t^{\text{ch}} \quad \forall t, \{\beta_t^{\text{ch}}\} \in \{0, 1\} \quad (8)$$

$$\frac{P_{l,d,t}^{\text{dis}} k_t \times \text{HR} \times 3600}{\eta \times \text{LHV} \times \varpi} \leq \xi^\varphi \beta_{l,t}^{\text{dis}} \quad \forall t, \forall l, \{\beta_{l,t}^{\text{dis}}\} \in \{0, 1\} \quad (9)$$

$$\beta_{l,t}^{\text{dis}} + \beta_t^{\text{ch}} \leq 1 \quad \forall t, \forall l, \{\beta_{l,t}^{\text{dis}}, \beta_t^{\text{ch}}\} \in \{0, 1\} \quad (10)$$

As discussed earlier, the charging status of the LNG storage (β_t^{ch}) is treated as a $\mathcal{H}\&\mathcal{N}$ decision because it is determined when the facility makes its decision regarding h_t . In contrast to β_t^{ch} (charging status of the LNG storage), $\beta_{l,t}^{\text{dis}}$ (discharging

status of the LNG storage) is a $\mathcal{W}\&\mathcal{S}$ decision and depends on the realization of LNG market scenarios. This implies that the facility first decides on the charging status of the LNG storage while submitting LNG bids and then decides on its discharging status, which coincides with its electricity generation mode ($P_{l,d,t}^{\text{dis}}$), as demonstrated in (9).

Constraints (11) and (12) establish the operational limits of the facility for selling and buying power through electricity offers and bids in the day-ahead market, respectively, by imposing distinct bounds for electricity discharging and charging:

$$\underline{P}_{l,d,t}^{\text{dis}} \alpha_{l,t}^{\text{dis}} \leq P_{l,d,t}^{\text{dis}} \leq \overline{P}_{l,d,t}^{\text{dis}} \alpha_{l,t}^{\text{dis}} \quad \forall t, \forall l, \forall d \quad (11)$$

$$\underline{P}_{l,d,t}^{\text{ch}} \alpha_{l,t}^{\text{ch}} \leq P_{l,d,t}^{\text{ch}} \leq \overline{P}_{l,d,t}^{\text{ch}} \alpha_{l,t}^{\text{ch}} \quad \forall t, \forall l, \forall d \quad (12)$$

The LAES plant is not allowed to be charged and discharged at the same time, as enforced below:

$$\alpha_{l,t}^{\text{dis}} + \alpha_{l,t}^{\text{ch}} \leq 1 \quad \forall t, \forall l, \{\alpha_{l,t}^{\text{dis}}, \alpha_{l,t}^{\text{ch}}\} \in \{0, 1\} \quad (13)$$

The liquid level of the liquid air tank in each time period is influenced by four factors: the previous period's liquid level, the tank's boil-off rate, the quantity of energy added to the tank by liquifying air, and the quantity of liquid air energy discharged from the tank and transferred to the expansion unit. During the facility's operation, the following equations are used to update the liquid level in the liquid air tank during the first and remaining periods:

$$q_{l,d,t}^{\text{LAES}} = q_0^{\text{LAES}} \left(1 - \frac{\mathcal{R}^{\text{LAES}}}{24} \right) + P_{l,d,t}^{\text{ch}} k_t - P_{l,d,t}^{\text{dis}} k_t \text{ER} \quad \forall t = 1, \forall l, \forall d \quad (14)$$

$$q_{l,d,t}^{\text{LAES}} = q_{l,d,t-1}^{\text{LAES}} \left(1 - \frac{\mathcal{R}^{\text{LAES}}}{24} \right) + P_{l,d,t}^{\text{ch}} k_t - P_{l,d,t}^{\text{dis}} k_t \text{ER} \quad \forall t \geq 2, \forall l, \forall d \quad (15)$$

It should be emphasized that the energy ratio (ER) in (14)-(15) serves as a measure of the system's efficiency, indicating the proportion of energy utilized for liquefaction to the energy generated during expansion. Constraint (16) ensures that the liquid level in the liquid air tank is equal to the level at the end of the dispatching horizon, whereas constraint (17) secures maintaining the liquid level within the designed limits:

$$q_{l,d,t}^{\text{LAES}} = q_0^{\text{LAES}} \quad \forall t = 24, \forall l, \forall d \quad (16)$$

$$\underline{Q}^{\text{LAES}} \leq q_{l,d,t}^{\text{LAES}} \leq \overline{Q}^{\text{LAES}} \quad \forall t, \forall l, \forall d \quad (17)$$

Last but not least, constraints (18)-(21) reflect the nonanticipativity of $\mathcal{H}\&\mathcal{N}$ and $\mathcal{W}\&\mathcal{S}$ decisions. In the given constraints, indices l, l' and d, d' represent two distinct scenarios from the scenario sets \mathcal{L} and \mathcal{D} , respectively. Considering two identical realizations of LNG prices in scenarios l and l' , the nonanticipativity constraints (18) and (19) enforce that facility's offers/bids at a given time period for both scenarios l and l' have to be the same. When the electricity price values are equal in scenarios d and d' , constraints (20) and (21) impose that the facility generates identical offering/bidding values for scenarios d and d' .

The electricity market operator has specified constraints (22) and (23) to enforce the necessity of offering and bidding curves with specific characteristics in the day-ahead electricity market. Constraint (22) ensures that offers made by market players must exhibit an increasing trend, while constraint (23) mandates a decreasing pattern for bids. These requirements maintain the desired market behavior and facilitate efficient price discovery. In general, constraints (20)-(23) enable the facility to accurately determine the optimal energy-price pairs that compose offering and bidding curves.

$$P_{l,d,t}^{\text{dis}} = P_{l',d,t}^{\text{dis}} \quad \text{if } \lambda_l^{\text{LNG}} = \lambda_{l'}^{\text{LNG}} \quad \forall t, \forall l, \forall l', d \quad (18)$$

$$P_{l,d,t}^{\text{ch}} = P_{l',d,t}^{\text{ch}} \quad \text{if } \lambda_l^{\text{LNG}} = \lambda_{l'}^{\text{LNG}} \quad \forall t, \forall l, \forall l', d \quad (19)$$

$$P_{l,d,t}^{\text{dis}} = P_{l,d',t}^{\text{dis}} \quad \text{if } \lambda_{d,t}^{\text{Elec}} = \lambda_{d',t}^{\text{Elec}} \quad \forall t, \forall l, \forall d, d' \quad (20)$$

$$P_{l,d,t}^{\text{ch}} = P_{l,d',t}^{\text{ch}} \quad \text{if } \lambda_{d,t}^{\text{Elec}} = \lambda_{d',t}^{\text{Elec}} \quad \forall t, \forall l, \forall d, d' \quad (21)$$

$$P_{l,d,t}^{\text{dis}} \geq P_{l,d',t}^{\text{dis}} \quad \text{if } \lambda_{d,t}^{\text{Elec}} \geq \lambda_{d',t}^{\text{Elec}} \quad \forall t, \forall l, \forall d, d' \quad (22)$$

$$P_{l,d,t}^{\text{ch}} \leq P_{l,d',t}^{\text{ch}} \quad \text{if } \lambda_{d,t}^{\text{Elec}} \geq \lambda_{d',t}^{\text{Elec}} \quad \forall t, \forall l, \forall d, d' \quad (23)$$

Note that variables $P_{l,d,t}^{\text{ch}}$ and $P_{l,d,t}^{\text{dis}}$ hold the index of electricity market scenarios d despite being $\mathcal{W}\&\mathcal{S}$ decisions, as the facility needs to submit offering and bidding curves instead of single values to the day-ahead electricity market. These variables may be referred to as “*special* $\mathcal{W}\&\mathcal{S}$,” although they are still classified as second-stage decision variables [38]. Summing up, variables h_t and β_t^{ch} are $\mathcal{H}\&\mathcal{N}$ decisions, whereas variables $\beta_{l,t}^{\text{dis}}, \alpha_{l,t}^{\text{ch}}, \alpha_{l,t}^{\text{dis}}, P_{l,d,t}^{\text{ch}}, P_{l,d,t}^{\text{dis}}, q_{l,d,t}^{\text{LNG}}$, and $q_{l,d,t}^{\text{LAES}}$ are $\mathcal{W}\&\mathcal{S}$ decisions in the proposed two-stage day-ahead dispatch model.

Fig. 4 illustrates the overall process of the LAES-LNG facility's dispatch in day-ahead LNG and electricity markets. Initially, input parameters such as market scenarios, technical parameters of the facility, and market specifications are fed into the optimization module (1)-(23). Through solving the optimization problem, the facility obtains the necessary information to determine the LNG bids and electricity offers/bids to be submitted to the respective markets. In practice, first, the facility submits the LNG bids (h_t) obtained from the optimization module. Upon releasing the LNG market results, the LAES-LNG facility decides on its offer/bid packages ($P_{l,d,t}^{\text{dis}}, P_{l,d,t}^{\text{ch}}$) in the electricity market.

IV. ECONOMIC FEASIBILITY STUDY: PROBABILISTIC PAYBACK PERIOD

When it comes to substantive deployment of the LAES-LNG facility in energy networks, investors and/or agencies are required to perform an economic feasibility study. Economic feasibility study is an analysis to check the viability of embarking on a project taking into account the costs and benefits. A key and primary component of such a study is the *payback period* metric, which measures how long it will take for an investment to turn into a profit (earn back its initial investment). To calculate an investment's *payback period*, G [year(s)], one must divide the total investment cost X [€] by annual profit Z [€/year], i.e., $G = \frac{X}{Z}$. While X and Z both follow random probability distributions, the probability density

$$f(g) = \frac{\sqrt{1-\rho^2}}{\pi\sigma_z\sigma_x a^2(g)} \exp\left(\frac{-m}{2(1-\rho^2)}\right) + \frac{b(g)n(g)}{2\sqrt{2\pi}\sigma_x\sigma_z a^3(g)} \left[\Theta\left(\frac{b(g)}{a(g)\sqrt{2(1-\rho^2)}}\right) - \Theta\left(\frac{-b(g)}{a(g)\sqrt{2(1-\rho^2)}}\right) \right]$$

where

$$a(g) = \sqrt{\frac{g^2}{\sigma_x^2} - \frac{2\rho g}{\sigma_x\sigma_z} + \frac{1}{\sigma_z^2}}, \quad b(g) = \frac{\mu_x g}{\sigma_x^2} - \frac{\rho(\mu_x + \mu_z g)}{\sigma_x\sigma_z} + \frac{\mu_z}{\sigma_z^2}, \quad m = \frac{\mu_x^2}{\sigma_x^2} - \frac{2\rho\mu_x\mu_z}{\sigma_x\sigma_z} + \frac{\mu_z^2}{\sigma_z^2}$$

$$n(g) = \exp\left(\frac{b^2(g) - ma^2(g)}{2(1-\rho^2)a^2(g)}\right), \quad \Theta(\psi) = \frac{2}{\sqrt{\pi}} \int_0^\psi \exp(-u^2) du \quad (24)$$

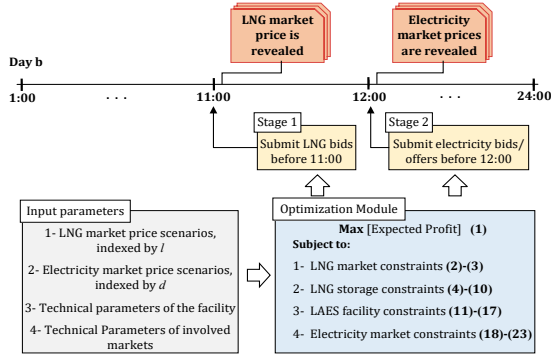


Fig. 4: High-level diagram of the day-ahead LAES-LNG dispatch.

function of G can be obtained through a number of techniques, including analytical, simulation, and statistical methods; however this work leverages a statistical method where X and Z follow Gaussian distributions [39]. This method, termed the Hinkley approach [39], estimates the probability distribution of G while treating both $X \sim \mathcal{N}(\mu_x, \sigma_x)$ and $Z \sim \mathcal{N}(\mu_z, \sigma_z)$ as correlated Gaussian distributions with mean and standard deviation denoted by μ and σ . The Hinkley method is a sound and computationally efficient estimating technique that can handle censored and uncensored data [40] without the need to know the correlation coefficient between X and Z , denoted by ρ^6 . This method yields equations (24) to estimate for the probability density function of *payback period*, $f(g)$. It is worth highlighting that the adopted approach is not limited to the *payback period* estimation but is a generic approach to estimating the probability distribution of any parameter defined by the division of two Gaussian distributions.

When (24) provides an estimate of the *payback period* probability distribution, other statistical features of $f(g)$, including mean μ_g [year(s)] and standard deviation σ_g [year(s)], can be derived as follows:

$$\mu_g = \int_{-\infty}^{+\infty} g f(g) dg \quad (25)$$

$$\sigma_g = \sqrt{\int_{-\infty}^{+\infty} (g - \mu_g)^2 f(g) dg} \quad (26)$$

For a broader economic feasibility analysis, beyond the *payback period*, there are other concrete measures such as net present value and internal rate of return [41]; however, these metrics are beyond the scope of this work.

⁶This coefficient takes values $-1 \leq \rho \leq +1$.

V. CASE STUDY

The financial gains of the proposed LAES-LNG dispatch model are evaluated in this section. Table I summarizes the technical characteristics of a LAES coupled with an LNG regasification process [27]. Note that the average USD-EUR exchange rate in 2021, 0.8458, was utilized to standardize all cost-related parameters [42]. The LAES-LNG facility is made up of an LNG storage and a liquid air tank with 217 m³ and 480 MWh capacities, an LNG regasification unit with 97% efficiency [43], and a LAES system with a discharge/charge rate of 122.2/60 MW. The lower bounds of the liquid level in both liquid air tank and LNG storage are established at 10% of their respective upper bounds [13]. Additionally, the initial liquid level is set slightly above the lower limit of the storage/tank. In line with [13], the lower limits for electricity charging and discharging are defined as 80% and 3% of their respective upper bounds. The LNG storage has a loading capacity of 16.19 m³/h, with an initial LNG level of 21.683 m³, to allow for a 12-hour filling time. The LNG lower heating value (LHV) and weight per unit volume (ϖ) are taken from [44] and [45], respectively. The facility is permitted to submit LNG bids between 10 and 20,000 MWh per day, as specified by the Iberian gas derivatives market. The formulation (1)-(23) possesses a mixed-integer linear structure. All results are derived by leveraging the CPLEX solver. Evidence that the proposed LAES-LNG model is cost-effective comes from:

- 1) a daily dispatch analysis versus an ideal freestanding LAES facility with high round-trip efficiency and a pragmatic freestanding LAES facility that is economically equivalent to the proposed LAES-LNG system. The numerical results are presented in subsection V-A.
- 2) an economic feasibility analysis based on actual market practice in 2021 and 2022 in the aftermath of market volatility induced by the recent energy crisis. The concerned analyses are discussed in subsection V-B.

A. Day-ahead Dispatch Study

Here, the cost-effectiveness of the LAES-LNG facility for a typical day is evaluated. Initially, one thousand distinct scenarios are generated for electricity and LNG prices using Gaussian distributions. It is assumed that electricity and LNG prices follow Gaussian distributions with mean values derived from the price data observed on January 21, 2021, and the standard deviation of recorded data throughout January 2021. Subsequently, leveraging SCENRED2 [47], the generated scenarios are reduced to ten (\mathcal{L}) and twenty-five (\mathcal{D}) delegate

TABLE I: Characteristics of the LAES-LNG facility.

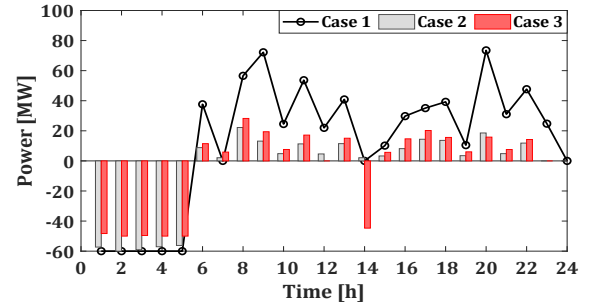
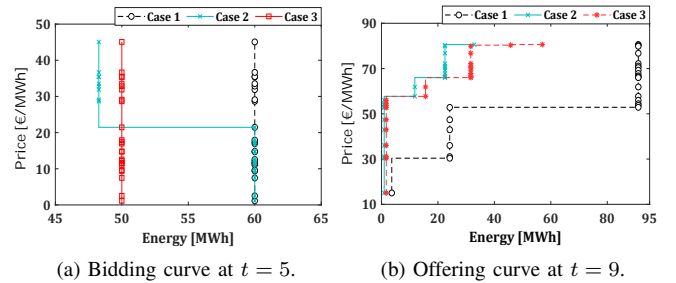
Parameter	Value	Unit	Parameter	Value	Unit
\mathcal{P}^{dis}	122.2	MW	q_0^{LAES}	50	MWh
$\overline{\mathcal{P}^{\text{dis}}}$	3.66	MW	$\overline{Q}^{\text{LNG}}$	217	m ³
$\overline{\mathcal{P}^{\text{ch}}}$	60	MW	$\underline{Q}^{\text{LNG}}$	21.7	m ³
$\underline{\mathcal{P}^{\text{ch}}}$	48	MW	q_0^{LNG}	21.863	m ³
ϑ^{dis}	3.72	€/MWh	$\xi^{\varphi}, \xi^{\ell}$	16.19	m ³ /h
ϑ^{ch}	3.72	€/MWh	η	0.97	-
$\mathcal{R}^{\text{LAES}}$	0.05	day ⁻¹	$\overline{\Psi}^{\text{LNG}}$	10	MWh
\mathcal{R}^{LNG}	0.05	day ⁻¹	$\underline{\Psi}^{\text{LNG}}$	20,000	MWh
$\overline{Q}^{\text{LAES}}$	480	MWh	HR	1.066	$\frac{\text{MWh}_{\text{thermal}}}{\text{MWh}_{\text{out}}}$
$\underline{Q}^{\text{LAES}}$	48	MWh	ER	0.491	$\frac{\text{MWh}_{\text{in}}}{\text{MWh}_{\text{out}}}$
LHV	48.6	MJ/kg	ϖ	457.4	kg/m ³

scenarios for LNG and electricity prices to feed the developed two-stage stochastic program. It is worth noting that the 25-block offering and bidding curves per hour required by the Iberian electricity market resulted in leveraging twenty-five scenarios for electricity prices. The following set of case studies is framed for a thorough analysis:

- **Case 1:** the proposed LAES-LNG facility with technical characteristics given in Table I [27].
- **Case 2:** a realistic freestanding LAES facility that is economically equivalent to **Case 1** [27]. The proposed LAES-LNG facility and the corresponding freestanding one should be examined under identical circumstances to provide a fair comparison of their respective economic feasibility. The technical specification of the realistic facility is listed in Table VIII, Appendix B. This case encompasses a facility with 55% round-trip efficiency, reduced operational expenses, and a lower discharge rate.
- **Case 3:** an ideal freestanding LAES facility with 70% round-trip efficiency and low operational costs, as proposed in [13]. Table VIII in Appendix B details the technical parameters of this case study, which are derived from [13].

A cautionary note is that both **Case 2** and **Case 3** track the mixed-integer formulation (27)-(38) outlined in Appendix A for the day-ahead dispatch.

The expected profit, total daily LNG bids, total expected daily electricity bids and offers, and all terms of objective functions (1) and (27) in different case studies are reported in Table II. The comparison between different case studies' expected profit indicates that the proposed LAES-LNG facility yields the highest profitability. Despite an expense of €15,164.19 LNG procurement from the day-ahead LNG market, the proposed facility offers substantially higher profit than that of two other freestanding systems by gaining a high revenue of €39,378.67 through selling power in the day-ahead electricity market. It is crucial to consider this issue due to the fact that the electricity market yields a maximum revenue of €14,357.76 for other freestanding systems. Further, results verify that the financial gain of the proposed LAES-LNG facility versus its economically equivalent freestanding system

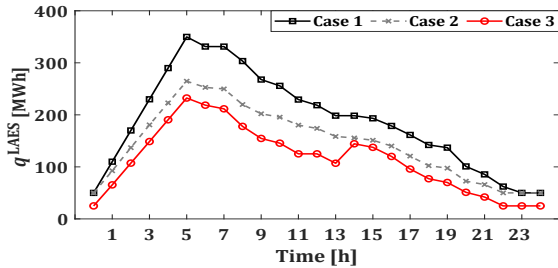
Fig. 5: Hourly electricity bids and offers in **Case 1-3**.Fig. 6: Day-ahead offer and bid curves in **Case 1-3** for two selected periods.

(**Case 2**) is 3.1 times higher, making it a much more competing option for grid deployment. **Case 1** create a 91.4% growth in profitability, even compared to the best-case scenario for LAES (**Case 3**), which features a round-trip efficiency of 70% and low operational costs. Not surprisingly, the proposed facility has more frequent dealings with electricity markets, as specifically shown in Fig. 5. This figure exhibits the detailed interaction of different case studies with electricity markets. Charging and discharging of all facilities tend to roughly follow the same pattern, with the main distinction arising at different levels of dealings. Even though the total expected daily bids of the proposed facility (**Case 1**) exceed those of the ideal freestanding system (**Case 3**), the cost of purchasing electricity for the ideal freestanding system is higher. This is attributed to the fact that in **Case 3**, the facility replenishes its charging power at $t = 14$ (due to the lower charging capacity) when the electricity price is higher. Offering and bidding curves in different case studies at two representative hours ($t = 5$ and $t = 9$) are depicted in Fig. 6. It is evident that offering curves exhibit a rising trend in both energy and price, indicating that as the energy level increases, so does the corresponding price. The opposite applies to the bidding curve. As an instance, the offering curve shows that for an electricity price of 70 €/MWh, the offering power of **Case 1** is roughly three times greater than that of other cases. Last but not least, Fig. 7 presents the liquid level of the liquid air tank for all case studies. With similar trends, the liquid air tank fills during the first periods and gradually releases while approaching the ending periods with higher electricity prices.

Driven by the promising economic performance of the established facility, two further case studies are set up to judge a determining parameter on its cost-effectiveness, i.e., loading

TABLE II: Expected profit, daily bought LNG, daily electricity bids and offers, and components of objective functions in **Case 1-3**.

Case Study	Profit [€]	$\sum_t P^{\text{dis}}$ [MWh]	$\sum_t P^{\text{ch}}$ [MWh]	H^{tot} [MWh]	$\sum_t \mathbb{E}[\mathcal{O}_1]$ [€]	$\sum_t \mathbb{E}[\mathcal{O}_2]$ [€]	$\sum_t \mathbb{E}[\mathcal{O}_3]$ [€]	$\sum_t \mathbb{E}[\mathcal{O}_4]$ [€]	$\sum_t \mathbb{E}[\mathcal{O}_5]$ [€]
Case 1	15,797.00	609.10	300.00	671.26	-15,164.19	39,378.67	-5,035.59	-2,265.87	-1,116.00
Case 2	4,976.84	158.77	289.66	—	—	10,797.81	-4,681.91	-403.29	-735.76
Case 3	8,252.50	204.62	292.57	—	—	14,357.76	-6,012.14	-27.03	-66.09

Fig. 7: Liquid level of the liquid air tank in **Case 1-3**.

(ξ^{φ}) and unloading (ξ^{ℓ}) capacities of the LNG storage:

- **Case 4**: a LAES-LNG facility with $\xi^{\varphi}, \xi^{\ell} = 12.95 \text{ m}^3/\text{h}$.
- **Case 5**: a LAES-LNG facility with $\xi^{\varphi}, \xi^{\ell} = 19.43 \text{ m}^3/\text{h}$.

Cases 4 and 5 assume a loading/unloading capacity of $\pm 20 \text{ MW/h}$ ($\pm 3.24 \text{ m}^3/\text{h}$) over **Case 1** ($\xi^{\varphi}, \xi^{\ell} = 16.19 \text{ m}^3/\text{h}$). Note that $3.24^7 \text{ m}^3/\text{h}$ loading/unloading LNG approximately equals to 20 MW/h input/output energy. The results arising from distinct loading/unloading capacities are outlined in Table III. The results manifest the inevitable impact of loading/unloading capacity on the facility's financial profit (bottom line). Indeed, the facility's bottom line can be increased by embedding cutting-edge machinery and infrastructure with higher loading and unloading rates. A further important insight gleaned from this table is that despite roughly equal overall interaction of the facility in **Case 1** and **Case 4** with electricity and LNG markets, $3.24 \text{ m}^3/\text{h}$ higher loading/unloading capacity yields €2,306.13 more profit. The details can be seen in Fig. 8. The reduced loading/unloading capacity causes the facility to acquire its target quantity of LNG across a greater number of periods, as shown by the blue bars (**Case 4**) compared to the green bars (**Case 1**). More specifically, the facility in **Case 4** acquires LNG during periods 6 and 15, as opposed to **Case 1**, to compensate for the LNG shortage. Lastly, the higher loading and unloading rates in **Case 5** yield greater interaction with the LNG market and a higher liquid level in total.

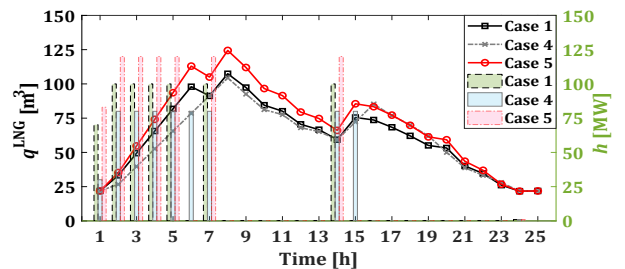
B. Economic Feasibility Study

Driven by the promising performance of the LAES-LNG facility in daily operation, this section is devoted to assessing the facility's economic feasibility focusing on the *payback period*. It is important to stress that both **Case 2** and **Case 3** (freestanding LAES facilities) failed to recoup their initial

$${}^7_{3.24} = \begin{cases} 16.19 - 12.95 \\ 19.43 - 16.19 \end{cases}$$

TABLE III: Expected profit, daily bought LNG, and daily electricity bids and offers in **Case 1, 4, and 5**.

Case Study	Profit [€]	$\sum_t P^{\text{dis}}$ [MWh]	$\sum_t P^{\text{ch}}$ [MWh]	H^{tot} [MWh]
Case 1	15,797.00	609.10	300.00	671.26
Case 4	13,490.87	608.99	300.00	671.07
Case 5	17,415.23	729.66	359.19	803.96

Fig. 8: Liquid level of LNG storage (lines) and LNG bids (bars) in **Case 1** and **Case 4** and **5**. The left and right y-axes correspond to lines and bars, respectively.

investment expenditures within their expected lifetimes (30 years); hence they did not undergo the economic feasibility study. **Case 4** is also overlooked; consequently, **Case 1** and **Case 5** are the focus of this section, given their competing economic prospect. Further, \mathcal{P}^{ch} and \mathcal{P}^{dis} are set to zero as these are design parameters that can be tackled in a demonstration plant.

Four primary parameters must be available to execute the probabilistic *payback period* based on the Hinkley approach described in Section IV: $\mu_x, \mu_z, \sigma_x,$ and σ_z . These four parameters correspond to the mean and standard deviation of the facility's total investment cost and annual profit, respectively. The mean investment cost of the LAES-LNG facility is set to €120.61e6 [27] while assuming 8% of the total investment cost as the standard deviation [46]. To acquire the mean and standard deviation of annual profit, this work relies on real-life electricity and LNG market prices in 2021 and 2022. These two specific time horizons are chosen to leverage the insight that the global rise of energy prices from 2021 onward altered the playground for market players. It is broadly deemed that surging global demand in the aftermath of the COVID-19 outbreak and Russia's assault on Ukraine are the key factors for such a salient shift. Fig. 9 depicts the electricity and LNG

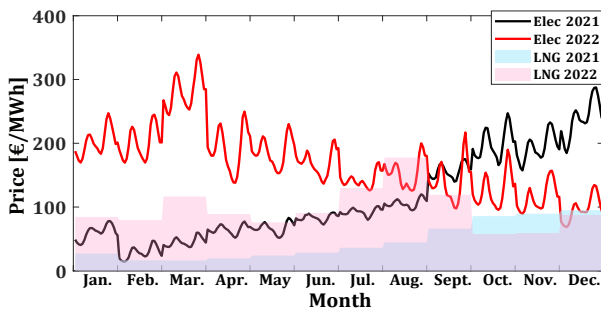


Fig. 9: 2021 and 2022 average electricity and LNG prices on a daily basis.

TABLE IV: Mean and standard deviation of the facility's profit over 2021 and 2022 under **Case 1**.

Profit	2021		2022	
	μ_z [€]	σ_z [€]	μ_z [€]	σ_z [€]
January	6.10e5	2.80e5	1.30e6	2.91e5
February	2.74e5	5.88e4	1.29e6	3.85e5
March	4.07e5	9.23e4	2.40e6	8.35e5
April	5.41e5	1.05e5	1.52e6	5.04e5
May	5.66e5	1.15e5	1.23e6	2.08e5
June	4.61e5	1.11e5	5.02e5	3.62e5
July	3.66e5	8.73e4	-8.99e3	4.49e3
August	4.10e5	1.15e5	-1.40e4	1.21e4
September	6.49e5	3.48e5	2.76e5	2.80e5
October	1.30e6	4.12e5	1.17e6	6.77e5
November	1.07e6	3.36e5	7.15e5	4.96e5
December	2.20e6	5.98e5	3.93e5	3.49e5
Annual	8.86e6	9.54e5	1.08e7	1.50e6

prices trajectory in 2021 and 2022 Iberian energy markets on a daily basis. Electricity and LNG prices rose steadily beginning in 2021 and continuing through the end of the year. Electricity prices continue to increase during the first quarter of 2022 and then start cutting down in the subsequent months. Conversely, LNG prices in 2022 track a stable trajectory during the first two quarters before skyrocketing in the third and then dropping through the final quarter.

As electricity prices rise, the disparity between peak and off-peak electricity prices widens. This provides an intriguing opportunity for energy storage stakeholders to engage in energy arbitrage practices. In light of this, we calculate the mean and standard deviation of the LAES-LNG annual profit for **Case 1** and **Case 5** over 2021 and 2022, and the results are reported in Table IV and Table V. To calculate the annual profit of the LAES-LNG facility, we adopt a procedure similar to that described in [48]. Initially, the statistical data is organized into 12 sets, each corresponding to a specific month. These sets are then further divided into 24 subsets for electricity prices, representing individual hours of the day, and 1 subset for LNG prices, representing a single price for the entire

TABLE V: Mean and standard deviation of the facility's profit over 2021 and 2022 under **Case 5**.

Profit	2021		2022	
	μ_z [€]	σ_z [€]	μ_z [€]	σ_z [€]
January	6.92e5	3.30e5	1.47e6	3.17e5
February	3.13e5	7.22e4	1.47e6	4.28e5
March	4.60e5	1.04e5	2.72e6	1.03e5
April	6.11e5	1.22e5	1.72e6	5.86e5
May	6.35e5	1.24e5	1.43e6	2.48e5
June	5.17e5	1.21e5	5.75e5	4.34e5
July	4.09e5	1.07e5	-8.99e3	4.49e3
August	4.65e5	1.19e5	-1.40e4	1.21e4
September	7.35e5	3.77e5	3.21e5	3.35e5
October	1.47e6	4.49e5	1.35e6	2.61e4
November	1.20e6	2.46e5	8.22e5	5.92e5
December	2.46e6	6.45e5	4.44e5	4.21e5
Annual	9.97e6	1.05e6	1.23e7	1.80e6

day. The subsets are then fitted to Gaussian distributions to derive 24 fits for electricity prices and 1 additional fit for LNG prices, corresponding to each month of the year. To characterize the uncertainties, the same scenario generation-reduction procedure outlined in section V-A is employed to derive the representative scenarios of LNG and electricity prices. Lastly, the representative scenarios are fed into the developed dispatch model in section III to obtain monthly and, accordingly, annual profit of the facility.

As can be seen, the fourth quarter of 2021 is the most profitable period for the LAES-LNG facility due to the dramatic increase in electricity prices. The facility reaps its greatest profits in December 2021 across that year. In 2022, however, the narrative shifts. The first half of 2022, with high electricity prices and relatively steady LNG prices, yields a paramount share of the facility's annual profit. Evidently, the facility makes a loss in July and August due to the spike in LNG prices and the drop in electricity prices (due to operational costs and technical constraints). Additionally, higher loading/unloading rates (**Case 5**) significantly impact yearly earnings, emphasizing the importance of meticulously selecting this value in the design process.

Given the above, the probability density function $f(g)$ (*payback period*) can be estimated by having four parameters μ_x , μ_z , σ_x , and σ_z . The probability density functions of the *payback period* derived from 2021 and 2022 market observations are displayed in Fig. 10 and Fig. 11. The probability density functions of the *payback period* derived from 2021 and 2022 market observations are displayed in Fig. 8 and Fig. 9 for two arbitrary correlation coefficients $\rho = 0.3$ and $\rho = 0.7$. Table VI and Table VII draw clear-cut probabilistic metrics of the *payback period*, namely, mean (μ_g) and standard deviation (σ_g). The last row of these tables represents the probability of reaching a *payback period* shorter than 15 years,

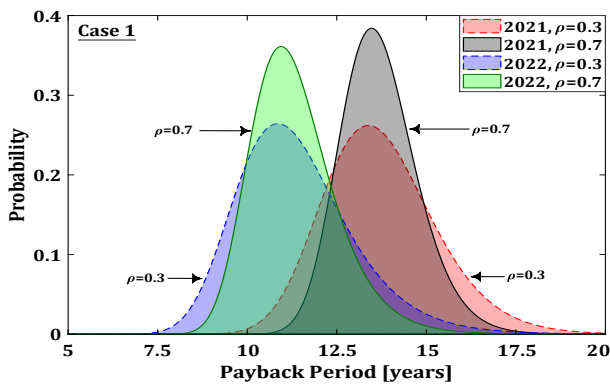


Fig. 10: Probability density function of the *payback period* derived from 2021 market observations.

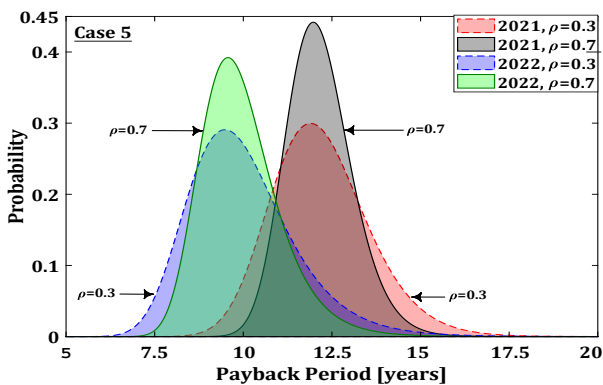


Fig. 11: Probability density function of the *payback period* derived from 2022 market observations.

half of the facility's lifetime. It can be inferred from these two tables that the mean *payback period* based on 2022 market observations is at least two years shorter than that of 2021. Moreover, a higher correlation coefficient yields a smaller standard deviation and, thus, a narrower probability density function. This can be interpreted as greater predictability and stability (lower uncertainty and greater confidence) while undergoing a higher correlation between investment cost and annual profit. In closing, it is very likely ($> 80\%$) and almost certain ($> 99\%$) that LAES-LNG will turn into a profit for its investors based on 2021 and 2022 projections, respectively. The above rewarding probabilistic metrics cannot be unearthed by leveraging a deterministic payback period study.

VI. CONCLUSION

This paper proposed the first day-ahead dispatch model for an LNG regasification unit coupled with a LAES facility interacting with LNG and electricity markets. The dispatch pattern was formulated as a two-stage stochastic setup with a linear setup given sequentially cleared LNG and electricity markets. Thanks to the TVB's readiness, the facility could actively interact with the LNG market, thus ensuring its stable functionality. The day-ahead dispatch model was tested against freestanding LAES models on a sample working day, and the results show that the established LAES-LNG facility reaped considerably higher profits than both economically equivalent freestanding facility and the highly efficient LAES system; the

TABLE VI: Probabilistic metrics of the *payback period* based on 2021 market observations.

Descriptive Statistics	Case 1		Case 5	
	$\rho=0.3$	$\rho=0.7$	$\rho=0.3$	$\rho=0.7$
μ_g [years]	13.5564	13.5803	12.0422	12.0628
σ_g [years]	1.5275	1.0414	1.3349	0.9052
$\mathcal{P}(g \leq 15)$ *	0.8277	0.9136	0.9866	0.9994

$$*\mathcal{P}(g \leq 15) = \int_0^{15} f(g) dg.$$

TABLE VII: Probabilistic metrics of the *payback period* based on 2022 market observations.

Descriptive Statistics	Case 1		Case 5	
	$\rho=0.3$	$\rho=0.7$	$\rho=0.3$	$\rho=0.7$
μ_g [years]	11.0983	11.1237	9.7185	9.7418
σ_g [years]	1.5167	1.1094	1.3788	1.0222
$\mathcal{P}(g \leq 15)$ *	0.9950	0.9998	0.9994	1.0000

$$*\mathcal{P}(g \leq 15) = \int_0^{15} f(g) dg.$$

loading/unloading capacity of the LNG storage is a decisive ingredient in the facility's bottom line.

What is more, this work went beyond the prior research leveraging Hinkley's approach and real-life market observations to conduct a probabilistic *payback period* analysis. Case studies on this economic feasibility study demonstrated that (i) the proposed LAES-LNG facility recouped its capital expenditures, while freestanding facilities did not; (ii) the *payback period* was found to be drastically influenced by the inspected time horizon; (iii) the executed analysis unearthed rewarding probabilistic metrics, excelling prior deterministic studies on the economic feasibility of LAES facilities.

Future works can be directed toward unveiling the thorough economic potential of the LAES-LNG facility by embedding ancillary services in the developed dispatch pattern. Exploring the strategic dispatch strategies of the facility within the electricity and LNG markets could be another promising area of research. Besides, a cutting-edge long-term forecasting tool for electricity and LNG prices can empower the developed economic feasibility study.

ACKNOWLEDGMENT

The authors express their gratitude to the associate editor and five reviewers for their comments and suggestions, which significantly contributed to the improvement of the manuscript submitted originally. This research was carried out in the context of the Energy Transition Fund, DISCRETE project, supported by the FPS Economy, S.M.E.s, Self-Employed and Energy, Belgium.

REFERENCES

- [1] T. Zhang, L. Chen, X. Zhang, S. Mei, X. Xue, and Y. Zhou, "Thermodynamic analysis of a novel hybrid liquid air energy storage system based on the utilization of LNG cold energy," *Energy*, vol. 155, pp. 641–650, Jul. 2018.

- [2] H. Qing, W. Lijian, Z. Qian, L. Chang, D. Dongmei, and L. Wenyi, "Thermodynamic analysis and optimization of liquefied air energy storage system," *Energy*, vol. 173, pp. 162–173, Apr. 2019.
- [3] A. A. Kebede, T. Kalogiannis, J. van Mierlo, and M. Berecibar, "A comprehensive review of stationary energy storage devices for large scale renewable energy sources grid integration," *Renewable and Sustainable Energy Reviews*, vol. 159, p. 112213, May 2022.
- [4] X. Peng et al., "Liquid air energy storage flexibly coupled with LNG regasification for improving air liquefaction," *Appl Energy*, vol. 250, pp. 1190–1201, Sep. 2019.
- [5] A. Vecchi, Y. Li, Y. Ding, P. Mancarella, and A. Sciacovelli, "Liquid air energy storage (LAES): A review on technology state-of-the-art, integration pathways and future perspectives," *Advances in Applied Energy*, vol. 3, p. 100047, Aug. 2021.
- [6] E. M. Smith, "Storage of Electrical Energy Using Supercritical Liquid Air," *Proceedings of the Institution of Mechanical Engineers*, vol. 191, no. 1, pp. 289–298, Jun. 1977.
- [7] K. Kishimoto, K. Hasegawa, and T. Asano, "Development of Generator of Liquid Air Storage Energy System," *Technical Review - Mitsubishi Heavy Industries*, vol. 35, no. 3, pp. 117–120, 1998.
- [8] T. Liang et al., "Liquid air energy storage technology: a comprehensive review of research, development and deployment," *Progress in Energy*, 2022.
- [9] "Plants — Highview Power." <https://highviewpower.com/plants/> (accessed Jun. 09, 2023).
- [10] "Vermont Liquid Air Energy Storage System, US." <https://www.power-technology.com/marketdata/vermont-liquid-air-energy-storage-system-us/> (accessed Jun. 09, 2023).
- [11] "Highview Power Developing 2 GWh of Liquid Air Long Duration Energy Storage Projects in Spain — Highview Power." https://highviewpower.com/news_announcement/highview-power-developing-2-gwh-of-liquid-air-long-duration-energy-storage-projects-in-spain/ (accessed Jun. 09, 2023).
- [12] "Chile's 50-MW/600-MWh LAES project wins approval." <https://renewablesnow.com/news/chiles-50-mw600-mwh-laes-project-wins-approval-796804/> (accessed Jun. 09, 2023).
- [13] H. Khani and M. R. Dadash Zadeh, "Real-Time Optimal Dispatch and Economic Viability of Cryogenic Energy Storage Exploiting Arbitrage Opportunities in an Electricity Market," *IEEE Trans Smart Grid*, vol. 6, no. 1, pp. 391–401, Jan. 2015.
- [14] C. Xie, Y. Hong, Y. Ding, Y. Li, and J. Radcliffe, "An economic feasibility assessment of decoupled energy storage in the UK: With liquid air energy storage as a case study," *Appl Energy*, vol. 225, pp. 244–257, Sep. 2018.
- [15] B. Lin, W. Wu, M. Bai, C. Xie, and J. Radcliffe, "Liquid air energy storage: Price arbitrage operations and sizing optimization in the GB real-time electricity market," *Energy Econ*, vol. 78, pp. 647–655, Feb. 2019.
- [16] A. Vecchi, J. Naughton, Y. Li, P. Mancarella, and A. Sciacovelli, "Multi-mode operation of a Liquid Air Energy Storage (LAES) plant providing energy arbitrage and reserve services – Analysis of optimal scheduling and sizing through MILP modelling with integrated thermodynamic performance," *Energy*, vol. 200, p. 117500, Jun. 2020.
- [17] A. Vecchi, Y. Li, P. Mancarella, and A. Sciacovelli, "Integrated techno-economic assessment of Liquid Air Energy Storage (LAES) under off-design conditions: Links between provision of market services and thermodynamic performance," *Appl Energy*, vol. 262, p. 114589, Mar. 2020.
- [18] M. Legrand, R. Labajo-Hurtado, L. M. Rodríguez-Antón, and Y. Doce, "Price arbitrage optimization of a photovoltaic power plant with liquid air energy storage. Implementation to the Spanish case," *Energy*, vol. 239, p. 121957, Jan. 2022.
- [19] Q. Zhang, I. E. Grossmann, C. F. Heuberger, A. Sundaramoorthy, and J. M. Pinto, "Air separation with cryogenic energy storage: Optimal scheduling considering electric energy and reserve markets," *AIChE Journal*, vol. 61, no. 5, pp. 1547–1558, May 2015.
- [20] F. Kong et al., "A Novel Economic Scheduling of Multi-Product Deterministic Demand for Co-Production Air Separation System with Liquid Air Energy Storage," *SSRN Electronic Journal*, 2022, doi: 10.2139/ssrn.4312875.
- [21] F. Kalavani, B. Mohammadi-Ivatloo, and K. Zare, "Optimal stochastic scheduling of cryogenic energy storage with wind power in the presence of a demand response program," *Renewable Energy*, vol. 130, pp. 268–280, 2019.
- [22] J. Park, S. Cho, M. Qi, W. Noh, I. Lee, and I. Moon, "Liquid air energy storage coupled with liquefied natural gas cold energy: Focus on efficiency, energy capacity, and flexibility," *Energy*, vol. 216, p. 119308, Feb. 2021.
- [23] M. Antonelli, S. Barsali, U. Desideri, R. Giglioli, F. Paganucci, and G. Pasini, "Liquid air energy storage: Potential and challenges of hybrid power plants," *Appl Energy*, vol. 194, pp. 522–529, May 2017.
- [24] T. H. Cetin, M. Kanoglu, and N. Yanikomer, "Cryogenic energy storage powered by geothermal energy," *Geothermics*, vol. 77, pp. 34–40, Jan. 2019.
- [25] M. H. Nabat, M. Soltani, A. R. Razmi, J. Nathwani, and M. B. Dusseault, "Investigation of a green energy storage system based on liquid air energy storage (LAES) and high-temperature concentrated solar power (CSP): Energy, exergy, economic, and environmental (4E) assessments, along with a case study for San Diego, US," *Sustain Cities Soc*, vol. 75, p. 103305, Dec. 2021.
- [26] P. Farres-Antunez, H. Xue, and A. J. White, "Thermodynamic analysis and optimisation of a combined liquid air and pumped thermal energy storage cycle," *J Energy Storage*, vol. 18, pp. 90–102, Aug. 2018.
- [27] J. Kim, Y. Noh, and D. Chang, "Storage system for distributed-energy generation using liquid air combined with liquefied natural gas," *Appl Energy*, vol. 212, pp. 1417–1432, Feb. 2018.
- [28] J. Park, S. Cho, M. Qi, W. Noh, I. Lee, and I. Moon, "Liquid air energy storage coupled with liquefied natural gas cold energy: Focus on efficiency, energy capacity, and flexibility," *Energy*, vol. 216, p. 119308, Feb. 2021.
- [29] X. Peng et al., "Liquid air energy storage flexibly coupled with LNG regasification for improving air liquefaction," *Appl Energy*, vol. 250, pp. 1190–1201, Sep. 2019.
- [30] B. Li, Y. Chen, W. Wei, Y. Hou, and S. Mei, "Enhancing resilience of emergency heat and power supply via deployment of LNG tube trailers: A mean-risk optimization approach," *Appl Energy*, vol. 318, p. 119204, Jul. 2022.
- [31] B. Li, Y. Chen, W. Wei, Z. Wang, and S. Mei, "Online Coordination of LNG Tube Trailer Dispatch and Resilience Restoration of Integrated Power-Gas Distribution Systems," *IEEE Trans Smart Grid*, vol. 13, no. 3, pp. 1938–1951, May 2022.
- [32] I. M. Trotter, M. F. M. Gomes, M. J. Braga, B. Brochmann, and O. N. Lie, "Optimal LNG (liquefied natural gas) regasification scheduling for import terminals with storage," *Energy*, vol. 105, pp. 80–88, Jun. 2016.
- [33] W. Wu, Y. Xiao, X. Wang, J. Wang, and X. Wang, "Operating Strategy of LNG Terminal in Interdependent Electricity and Natural Gas Markets," *IEEE Transactions on Energy Markets, Policy and Regulation*, pp. 1–13, 2023.
- [34] H. Khaloie, M. Mollahassani-Pour, and A. Anvari-Moghaddam, "Optimal Behavior of a Hybrid Power Producer in Day-Ahead and Intraday Markets: A Bi-Objective CVaR-Based Approach," *IEEE Trans Sustain Energy*, vol. 12, no. 2, pp. 931–943, Apr. 2021.
- [35] Z. Bodie, A. Kane, and A. J. Marcus, *Investments*. Boston: McGraw-Hill/Irwin, 2009.
- [36] A. Cukierman, "The effects of uncertainty on investment under risk neutrality with endogenous information," *Journal of Political Economy*, vol. 88, no. 3, pp. 462–475, 1980.
- [37] M. H. DeGroot and M. J. Schervish, *Probability and statistics*. Pearson Education, 2012.
- [38] H. Khaloie, F. Vallée, C. S. Lai, J.-F. Toubeau, and N. D. Hatzigiorgiou, "Day-ahead and intraday dispatch of an integrated biomass-concentrated solar system: A multi-objective risk-controlling approach," *IEEE Trans. Power Syst.*, vol. 37, no. 1, pp. 701–714, Jan. 2022.
- [39] D. V. Hinkley, "On the ratio of two correlated normal random variables," *Biometrika*, vol. 56, no. 3, pp. 635–639, 1969.
- [40] J. F. Lawless, *Statistical models and methods for lifetime data*. John Wiley & Sons, 2011.
- [41] H. Khaloie, J.-F. Toubeau, F. Vallee, C. S. Lai, and L. L. Lai, "An Innovative Coalitional Trading Model for a Biomass Power Plant Paired With Green Energy Resources," *IEEE Trans Sustain Energy*, vol. 13, no. 2, pp. 892–904, Apr. 2022.
- [42] "US Dollar to Euro Spot Exchange Rates for 2021." <https://www.exchangerates.org.uk/USD-EUR-spot-exchange-rates-history-2021.html> (accessed May 24, 2023).
- [43] X. Wang and M. Economides, "CHAPTER 6 - Liquefied Natural Gas (LNG)," in *Advanced Natural Gas Engineering*, X. Wang and M. Economides, Eds., Gulf Publishing Company, 2009, pp. 209–241. doi: <https://doi.org/10.1016/B978-1-933762-38-8.50013-7>.
- [44] "Fuels - Higher and Lower Calorific Values." https://www.engineeringtoolbox.com/fuels-higher-calorific-values-d_169.html (accessed May 24, 2023).

- [45] A. BATTISTELLI, "Boil off gas handling on LNG fuelled vessels with high pressure gas injected engines," 2015, <https://www.politesi.polimi.it/handle/10589/116691> (accessed May 24, 2023).
- [46] G. Rothwell, "Cost contingency as the standard deviation of the cost estimate," *COST ENGINEERING-ANN ARBOR THEN MORGANTOWN*, vol. 47, no. 7, p. 22, 2005.
- [47] "SCENRED2." https://www.gams.com/latest/docs/T_SCENRED2.html (accessed Jun. 22, 2023).
- [48] R. Atia and N. Yamada, "Sizing and Analysis of Renewable Energy and Battery Systems in Residential Microgrids," *IEEE Trans Smart Grid*, vol. 7, no. 3, pp. 1204–1213, May 2016.

APPENDIX A

This section gives the day-ahead dispatch formulation of the freestanding LAES facility. With an objective function (27) and operational restrictions (28)-(38), the day-ahead dispatch formulation of the freestanding LAES facility displayed in Fig. 1 is presented below.

$$\begin{aligned} \text{Max } \mathbb{E} \mathcal{F}(y, \theta_d) = \sum_{t \in \mathcal{T}} \left[\mathbb{E}_{\mathcal{H} \& \mathcal{N}} \left[\underbrace{P_{d,t}^{\text{dis}} k_t \lambda_{d,t}^{\text{Elec}}}_{\mathcal{O}_2} - \underbrace{P_{d,t}^{\text{ch}} k_t \lambda_{d,t}^{\text{Elec}}}_{\mathcal{O}_3} \right. \right. \\ \left. \left. - \underbrace{P_{d,t}^{\text{dis}} k_t \vartheta^{\text{dis}}}_{\mathcal{O}_4} - \underbrace{P_{d,t}^{\text{ch}} k_t \vartheta^{\text{ch}}}_{\mathcal{O}_5} \right] \right] \end{aligned} \quad (27)$$

where terms \mathcal{O}_2 - \mathcal{O}_5 respectively correspond to terms \mathcal{O}_2 - \mathcal{O}_5 in (1).

$$\underline{P}_{d,t}^{\text{dis}} \alpha_t^{\text{dis}} \leq P_{d,t}^{\text{dis}} \leq \overline{P}_{d,t}^{\text{dis}} \alpha_t^{\text{dis}} \quad \forall t, \forall d \quad (28)$$

$$\underline{P}_{d,t}^{\text{ch}} \alpha_t^{\text{ch}} \leq P_{d,t}^{\text{ch}} \leq \overline{P}_{d,t}^{\text{ch}} \alpha_t^{\text{ch}} \quad \forall t, \forall d \quad (29)$$

$$\alpha_t^{\text{dis}} + \alpha_t^{\text{ch}} \leq 1 \quad \forall t, \{\alpha_t^{\text{dis}}, \alpha_t^{\text{ch}}\} \in \{0, 1\} \quad (30)$$

$$\begin{aligned} q_{d,t}^{\text{LAES}} = q_0^{\text{LAES}} \left(1 - \frac{\mathcal{R}^{\text{LAES}}}{24} \right) + P_{d,t}^{\text{ch}} k_t \sqrt{\eta^{\text{ETF}}} - \frac{P_{d,t}^{\text{dis}} k_t}{\sqrt{\eta^{\text{ETF}}}} \\ \forall t = 1, \forall d \end{aligned} \quad (31)$$

$$\begin{aligned} q_{d,t}^{\text{LAES}} = q_{d,t-1}^{\text{LAES}} \left(1 - \frac{\mathcal{R}^{\text{LAES}}}{24} \right) + P_{d,t}^{\text{ch}} k_t \sqrt{\eta^{\text{ETF}}} - \frac{P_{d,t}^{\text{dis}} k_t}{\sqrt{\eta^{\text{ETF}}}} \\ \forall t \geq 2, \forall d \end{aligned} \quad (32)$$

$$q_{d,t}^{\text{LAES}} = q_0^{\text{LAES}} \quad \forall t = 24, \forall d \quad (33)$$

$$\underline{Q}^{\text{LAES}} \leq q_{d,t}^{\text{LAES}} \leq \overline{Q}^{\text{LAES}} \quad \forall t, \forall d \quad (34)$$

$$P_{d,t}^{\text{dis}} = P_{d',t}^{\text{dis}} \quad \text{if } \lambda_{d,t}^{\text{Elec}} = \lambda_{d',t}^{\text{Elec}} \quad \forall t, \forall d, d' \quad (35)$$

$$P_{d,t}^{\text{ch}} = P_{d',t}^{\text{ch}} \quad \text{if } \lambda_{d,t}^{\text{Elec}} = \lambda_{d',t}^{\text{Elec}} \quad \forall t, \forall d, d' \quad (36)$$

$$P_{d,t}^{\text{dis}} \geq P_{d',t}^{\text{dis}} \quad \text{if } \lambda_{d,t}^{\text{Elec}} \geq \lambda_{d',t}^{\text{Elec}} \quad \forall t, \forall d, d' \quad (37)$$

$$P_{d,t}^{\text{ch}} \leq P_{d',t}^{\text{ch}} \quad \text{if } \lambda_{d,t}^{\text{Elec}} \geq \lambda_{d',t}^{\text{Elec}} \quad \forall t, \forall d, d' \quad (38)$$

where $\sqrt{\eta^{\text{ETF}}}$ is the LAES round-trip efficiency. Constraints (28)-(34) are mapped to constraints (11)-(17), respectively, and constraints (35)-(38) are analogous to the previously discussed constraints (20)-(23).

APPENDIX B

Technical parameters of benchmark LAES facilities corresponding to **Case 2** and **Case 3** are summarized in Table VIII and Table IX, respectively.

TABLE VIII: Technical specification of the freestanding LAES facility in **Case 2**.

Parameter	Value	Unit	Parameter	Value	Unit
$\overline{P}^{\text{dis}}$	32.9	MW	$\mathcal{R}^{\text{LAES}}$	0.5	%/day
$\underline{P}^{\text{dis}}$	0.987	MW	$\overline{Q}^{\text{LAES}}$	480	MWh
\overline{P}^{ch}	60	MW	$\underline{Q}^{\text{LAES}}$	48	MWh
$\underline{P}^{\text{ch}}$	48	MW	q_0^{LAES}	50	MWh
ϑ^{dis}	2.54	€/MWh	η^{RTE}	55	%
ϑ^{ch}	2.54	€/MWh	-	-	-

TABLE IX: Technical specification of the freestanding LAES facility in **Case 3**.

Parameter	Value	Unit	Parameter	Value	Unit
$\overline{P}^{\text{dis}}$	57	MW	$\mathcal{R}^{\text{LAES}}$	0.15	%/day
$\underline{P}^{\text{dis}}$	1.71	MW	$\overline{Q}^{\text{LAES}}$	247	MWh
\overline{P}^{ch}	50	MW	$\underline{Q}^{\text{LAES}}$	24.7	MWh
$\underline{P}^{\text{ch}}$	40	MW	q_0^{LAES}	25	MWh
ϑ^{dis}	0.2259	€/MWh	η^{RTE}	70	%
ϑ^{ch}	0.1321	€/MWh	-	-	-



Hooman Khaloie (Graduate Student Member, IEEE) received the M.Sc. degree (First Class Hons.) from Shahid Bahonar University of Kerman, Kerman, Iran, in 2019. He is currently a Researcher with PSMR Group at the University of Mons, Belgium. In 2020, he received an Outstanding Reviewer Award from the IEEE Transactions on Power Systems and was recognized for a Highly Cited Research Paper by Applied Energy. His research interests lie at the intersection of emerging energy technologies, energy markets, financial risk assessment, and data-driven

methods for energy applications.



François Vallée (Member, IEEE) received the degree in civil electrical engineering and the Ph.D. degree in electrical engineering from the Faculty of Engineering, University of Mons, Belgium, in 2003 and 2009, respectively. He is currently a Professor and leader of the "Power Systems and Markets Research Group" at the University of Mons. His Ph.D. work has been awarded by the SRBE/KBVE Robert Sinave Award in 2010. His research interests include PV and wind generation modeling for electrical system reliability studies in presence of dispersed

generation.